Multiphysics Modelling of Low Magnetic Curie Point Materials

Hakim Oueslati[1,2], Didier Trichet[1], Guillaume Wasselynck[1], and Simon Morville[2]

[1] Nantes University, Institut de Recherche en Energie Electrique de Nantes Atlantique, 37, Bd de l'université, Saint-Nazaire 44612, France

[2] Institut de Recherche Technologique Jules Verne, 1 Mail des 20 000 lieux, 44340 Bouguenais, France

Controlled Curie point materials are considered innovative materials due to their property of abrupt magnetic extinction when their temperature exceeds a specific threshold. This property makes them very suitable for a variety of industrial processes that require temperature self-regulation. The use of these materials in induction heating may allow the power transfer to be interrupted at an adjustable temperature, ensuring precise control of the heating process. The ability to adjust the Curie point temperature is a key advantage of these materials, as it allows custom solutions to be developed for specific industrial applications.
A coupled electromagnetic and thermal 1D model for induction heating of magnetic material with a low Curie point temperature is presented.
Curie temperature, Ferromagnetism, Magnetothermal coupling.

I. INTRODUCTION

IN recent years, metallurgists have developed so-called "controlled Curie point" materials. These materials have the property of magnetic extinction when their temperature exceeds a certain threshold. Energy transfer by electromagnetic induction could be greatly reduced in these areas, opening the door to thermal self-regulation of the process without sensors and only in the zones of interest (with low energy) [1]-[2]. This threshold is usually $800°C$ for steel, but there are now also materials whose threshold is set during manufacture in the range from ambient to $800°C$. This temperature range opens interesting perspectives for the production of thermoplastic (preforming, forming, welding, ...) and thermoset composites (polymerization, recycling, ...).
The main objective is to evaluate the potential of integrating these materials in the elaboration processes of glass or carbon fiber composites widely used in aeronautical and space industries through the implementation of a multiphysics and multiscale finite element code that integrates the strong magneto-thermal coupling of the phenomena associated with the crossing of the Curie point.

II. MATHEMATICAL MODELING

The management of the magnetic non-linearity as well as the abrupt change in the magnetic properties confronts us with meshing difficulties. Therefore, a simplification of the geometry and a switch to 1D can be useful to find an optimal strategy for magneto-thermal coupling and to reduce the high simulation time.

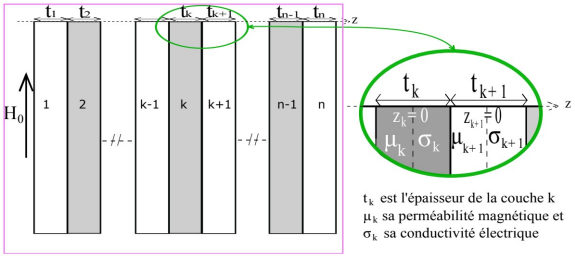

FIG. 1. Configuration of a multilayer 1D simulation

A one-dimensional multiphysics analytical tool for the electromagnetic part and a numerical tool for the thermal part is used to model the behavior of Curie point materials in the case of induction heating [3]. By combining Maxwell's equations, in the harmonic regime, and by considering that H varies according to a single axis z, we obtain the following H equation :

$$\frac{\partial}{\partial z}\left(\frac{1}{\sigma}\frac{\partial H}{\partial z}\right) - jw\mu H = 0 \tag{1}$$

The H-field equation is solved in each layer k of the material in the local reference system, where the origin is the middle of the layer. The solution, in each layer, of the magnetic field of equation 1 can be written as follows :

$$H_k(z) = A_k e^{-\gamma_k z} + B_k e^{\gamma_k z} \quad \text{avec} \quad \gamma_k = \frac{(1+j)}{\delta_k} \tag{2}$$

with δ_k the depth penetration of the layer k defined by :

$$\delta_k = \sqrt{\frac{2}{w\sigma_k\mu_k}}$$

By solving the differential equation in H, we obtain the distribution of the magnetic field at any point of the system. From there, we can deduce the other electromagnetic parameters such as the power density that will be injected into the thermal model.

$$q(z) = \frac{\|J(z)\|^2}{\sigma}$$

where

$$J(z) = \frac{\partial H(z)}{\partial z} = -\gamma A e^{-\gamma z} + \gamma B e^{\gamma z}$$

Knowing that the temperature varies along the z axis, the heat equation can be written as follows :

$$q(z) = -\frac{\partial\lambda(z)}{\partial z}\cdot\frac{\partial T_z^t}{\partial z} - \lambda(z)\cdot\frac{\partial^2 T_z^t}{\partial z^2} + \rho(z)\cdot C_p(z)\cdot\frac{\partial T_z^t}{\partial t} \tag{3}$$

The finite difference method is used to solve the thermal equation and takes into account the jumps in physical properties at the interface of the different layers. A discretization of layer thickness in Δz and time in Δt is required.

$$q(z) = -\frac{(\lambda_z - \lambda_{z-\Delta z})}{\Delta z}\cdot\frac{\left(T_z^t - T_{z-\Delta z}^t\right)}{\Delta z} - \lambda(z)\cdot\frac{T_{z+\Delta z}^t + T_{z-\Delta z}^t - 2T_z^t}{(\Delta z)^2} + \rho(z)\cdot C_p(z)\cdot\frac{\left(T_z^t - T_z^{t-\Delta t}\right)}{\Delta t} \tag{4}$$

By posing

$$e_z = \frac{\rho_z\cdot C_{p.z}}{\Delta t}, f_z = \frac{(\lambda_z + \lambda_{z-\Delta z})}{(\Delta z)^2} + e_z, \tag{5}$$

$$g_z = -\frac{\lambda_{z-\Delta z}}{(\Delta z)^2} \text{ et } h_z = -\frac{\lambda_z}{(\Delta z)^2}, \tag{6}$$

we obtain :

$$q_z + e_z\cdot T_z^{t-\Delta t} = f_z\cdot T_z^t + g_z\cdot T_{z-\Delta z}^t + h_z\cdot T_{z+\Delta z}^t \tag{7}$$

At both ends (1 and n) of the material, we have the following forced thermal convection boundary conditions :

$$\begin{cases} -\lambda_1 \cdot \frac{T_1 - T_2}{\Delta z} = h_G \left(T_1 - T_a\right) \\ -\lambda_n \cdot \frac{T_n - T_{n-1}}{\Delta z} = h_D \left(T_n - T_a\right) \end{cases} \quad (8)$$

In this work, we assume that at time $t = 0$, the temperature at any point in the system is equal to the ambient temperature.

III. NUMERICAL METHODOLOGY

III-A. Magnetothermal coupling

Magnetothermal coupling is an important phenomenon that occurs in many electromagnetic heating applications, including induction heating. In induction heating, an alternating electromagnetic field is used to heat a conductive material without any direct contact, which makes it an efficient and precise heating method for many industrial processes. However, the high-frequency electromagnetic field can also induce eddy currents in the material being heated, which in turn can produce heat due to the resistance of the material. This heat generation, known as the Joule effect, can be further enhanced by the magnetic properties of the material and its surrounding environment, which can lead to additional heating due to magnetothermal coupling.

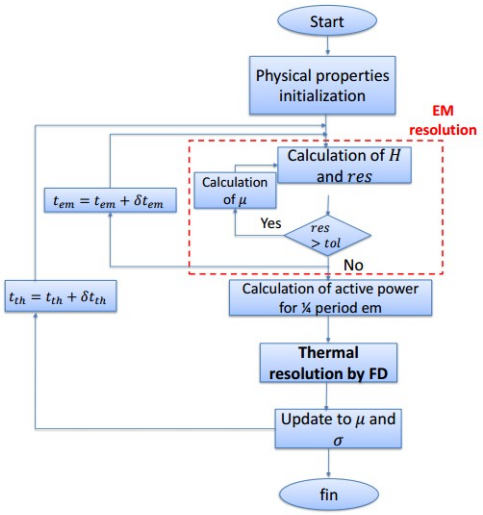

FIG. 2. Magnetothermal coupling algorithm

The average active power over an electromagnetic period is calculated as follows :

$$P_a = \frac{1}{T} \int_0^T p(t) dt$$

III-B. Material

Ferromagnetic $Fe-Ni-Cr$ austenitic alloys with less than $50\% Ni$ have a Curie point T_C that varies continuously with composition between $0°C$ and $500°C$ [4]-[5]. The material chosen for the numerical simulation is a ferromagnetic material with a Curie temperature $T_C = 280°C$. It is a saturable material whose relative magnetic permeability is not constant but depends on magnetic field H and temperature T. This double non-linearity is one of the modeling constraints to overcome. In saturable materials, the relative permeability increases with H to a maximum, then as it approaches saturation inverts and decreases toward 1. Also, Its magnetization curve $B(H)$ decreases progressively (Fig. 3) as the temperature T approaches T_C.
It should be noted that the permeability of ferromagnetic materials is very high at ambient temperature, which favors the generation of induced currents by attracting and concentrating magnetic flux lines. This property is essential in the generation of induced currents because the greater the magnetic flux density is, the stronger the induced current is. Therefore, a material with a high magnetic permeability can attract and retain more magnetic flux lines, making it easier to generate induced currents. As shown in Fig. 3, the magnetic field at the different temperatures does not exceed 800 (A/m) and μ_r is still far from reaching a value close to 1, as can be seen from Table I.

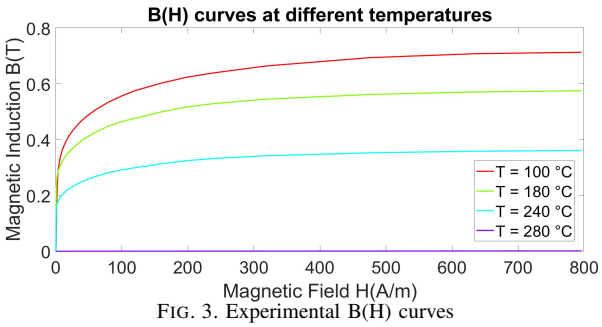

FIG. 3. Experimental B(H) curves

TABLE I. Magnetic characteristics of the material at different temperatures ($<$ and $>$ T_C)

	$H_{sat}(A/m)$	$B_{sat}(T)$	μ_{rsat}
$T = 100°C < T_C$	795.8	0.7	713
$T = 180°C < T_C$	795.8	0.6	575
$T = 240°C < T_C$	795.8	0.4	361
$T = 280°C > T_C$	795.8	10^{-3}	1

It is, therefore, necessary to extrapolate the experimental values to reach a complete magnetic saturation where $\mu_r \simeq 1$ [6] or to use an analytical model that describes the behavior of the experimental $B(H)$ curves which is the case here since we will use the Jiles-Atherton Model [7].

Fig. 3 shows the experimental magnetization curves of the ferromagnetic material at various temperatures. It can be seen that when the Curie temperature is exceeded $(T = 280°C = T_C)$ $\mu_r = 1$ and thus $B = \mu_0 \times H$.

By exploiting the experimental data, the parameters of the Jiles-Atherton model are explicitly identified. This helps us to achieve relatively high magnetic field values.
In an induction heating system, the frequency used is generally in the kilohertz (kHz) to tens of kilohertz range.

The magnetic field is directly related to the frequency used. The higher the frequency, the higher the magnetic field required to achieve sufficient heating efficiency. The typical magnetic field used can vary but is generally in the order of a few milliteslas (mT) to a few tens of milliteslas.

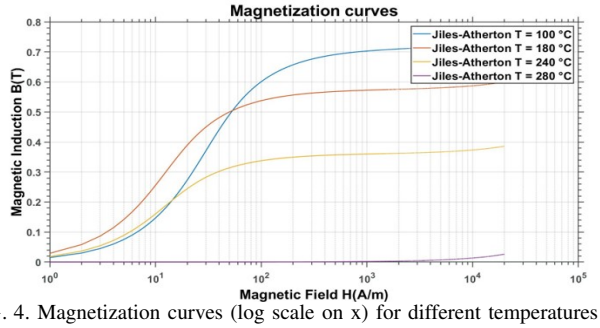

FIG. 4. Magnetization curves (log scale on x) for different temperatures ($<$ and $>$ T_C) according to the JA model

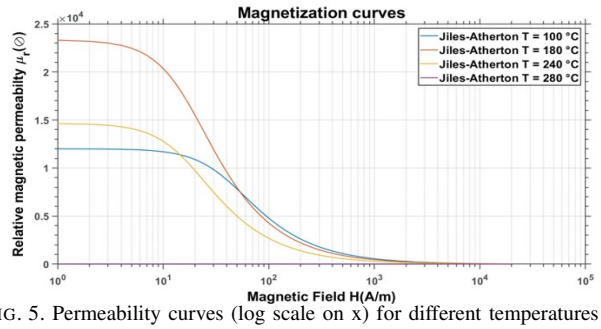

FIG. 5. Permeability curves (log scale on x) for different temperatures ($<$ and $>T_C$) according to the JA model

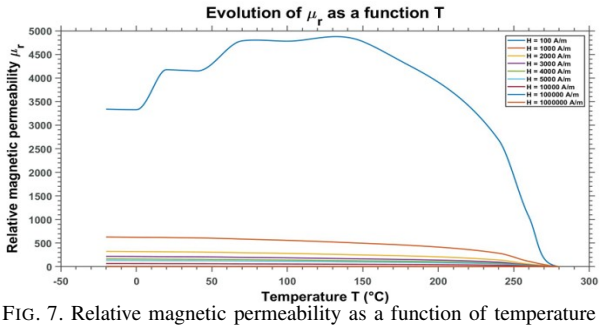

FIG. 7. Relative magnetic permeability as a function of temperature at different H values

As shown in Fig. 4 and Fig. 5, magnetization and permeability curves are available for fairly high magnetic field values, up to $20,000$ A/m.

III-C. Numerical results

The parameters used for the simulation are listed below :

TABLE II. General model parameters

Thickness of the plate	10 mm
Frequency f	1 MHz
Number of layers	5000
Curie point T_C	$280°C$

TABLE III. Electromagnetic model parameters

Permeability μ	$\mu(H,T)$
Electrical conductivity σ	5.10^6 S · m^{-1}
Final em time	$\frac{T}{4} = \frac{4}{f} = 2.5 \times 10^{-7}$ s
Number of steps	10
Time step	2.5×10^{-8} s

TABLE IV. Thermal model parameters

Density ρ	8200 Kg.m^{-3}
Conductivity λ	13 W.m^{-1}.K^{-1}
Heat C_p	500 J · Kg^{-1}.K^{-1}
Final th time	300 s
Number of steps	150
Time step	2 s

Since magnetic permeability is temperature-dependent, μ_r values must be acquired as a function of temperature at any magnetic field H value. A temperature range from -20 up to the Curie temperature is selected, in $1°C$ steps.

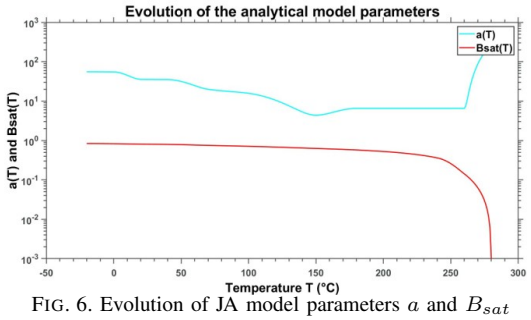

FIG. 6. Evolution of JA model parameters a and B_{sat}

From the values in Fig. 6 and the anhysteretic equation of the Jiles-Atherton model, curves of magnetic permeability versus temperature (Fig. 7) are constructed.

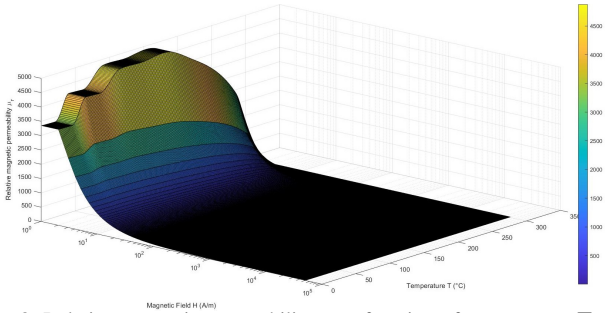

FIG. 8. Relative magnetic permeability as a function of temperature T and field H

Fig. 8 shows the decrease of the relative magnetic permeability as a function of both temperature and magnetic field.
I chose to present the active power density curve at several thermal iterations and at a frequency of 60 kHz and a source field of 10000 A/m.

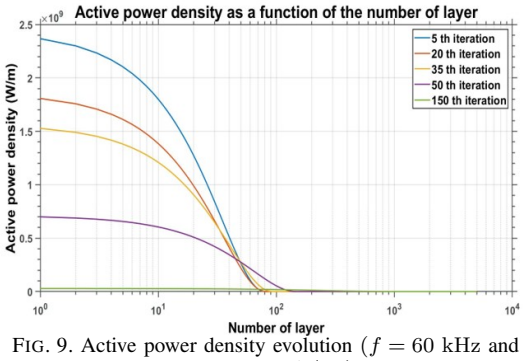

FIG. 9. Active power density evolution ($f = 60$ kHz and $H = 10000$ A/ m)

As shown in Fig. 9, we can see that the power density decreases as a function of the layer number, thus the existence of a skin effect. By heating the plate, the power density decreases and we can see that it becomes very low at the end of the heating where we surely reach the Curie temperature.
As confirmed in Fig. 10, the active power decreases with the heating time and increases with the source magnetic field.

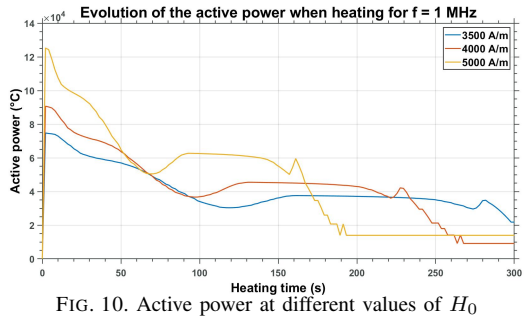

FIG. 10. Active power at different values of H_0

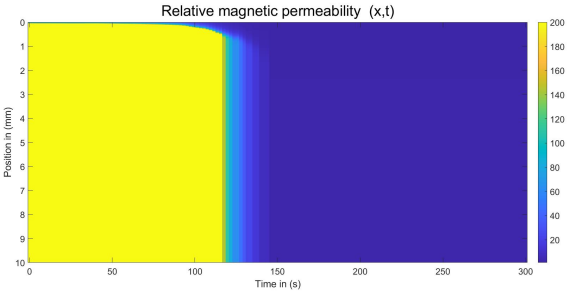

FIG. 11. Relative permeability distribution ($f = 60$ kHz, $H = 10000\ \ \mathrm{A.m^{-1}}$)

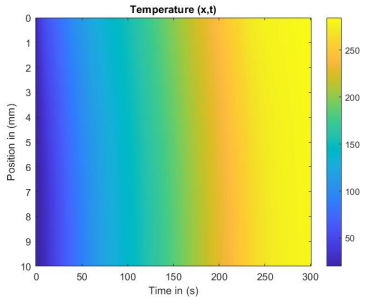

FIG. 12. Temperature distribution ($f = 60$ kHz, $H = 10000\ \ \mathrm{A.m^{-1}}$)

At these same parameters, the magnetic permeability becomes constant at about 1 mm from the plate, and from there we observe the phenomenon of magnetic saturation.
As can be seen from Fig. 11, the permeability which depends on the field and the temperature tends towards 1 when magnetic saturation is reached and also when the temperature exceeds the Curie temperature.
However, it decreases as a function of the heating time and tends to 1 when passing the Curie point.
The Curie temperature is reached more quickly when the magnetic field is increased. Fig. 12 shows the temperature distribution in the plate throughout the heating process.

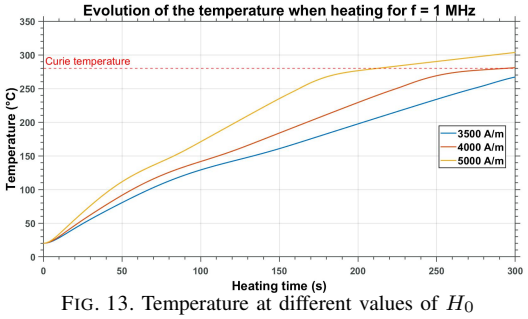

FIG. 13. Temperature at different values of H_0

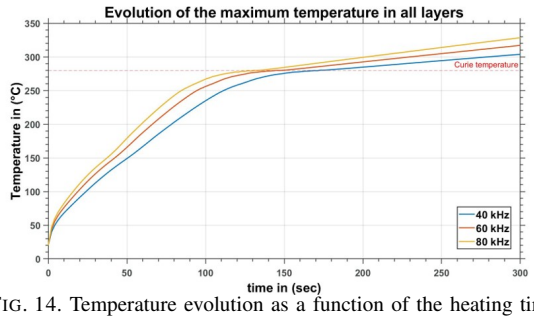

FIG. 14. Temperature evolution as a function of the heating time

The passage through the Curie point results in a stabilization of the active power which can be seen in the change of slope in the temperature curves (Fig. 13). Fig. 14 shows us the influence of the frequency and that when we increase the frequency, we reach the Curie temperature more quickly. What interests us most is the change in the slope of the temperature curve and this shows that we could indeed be looking for a temperature self-regulation since this change in slope proves that the induced power has strongly decreased at the passage of the Curie point but remains higher than the losses. Having a balance between induced power and losses will guarantee a constant temperature at the passage of the Curie point and thus temperature self-regulation.

IV. CONCLUSION

In this paper, a 1D coupled electromagnetic and thermal model, taking into account the non-linear magnetic characteristics of ferromagnetic materials, has been presented. The break of slope in the temperature curve at the Curie point makes the thermal self-regulation phenomenon exploitable.
Moving to a 2D model where we solve the electromagnetic and thermal problems by finite elements is the next step to be taken but it will not be as simple as in 1D. Since these innovative materials have magnetic properties that change abruptly, we must expect meshing problems. Also, simulation times will increase considerably.

ACKNOWLEDGMENT

This work is part of the PERFORM Program managed by IRT Jules Verne (French Institute in Research and Technology in Advanced Manufacturing Technologies for Composite, Metallic, and Hybrid Structures).

REFERENCES

[1] T. Todaka, T. Kishino, and M. Enokizono, “Low Curie temperature material for induction heating self-temperature controlling system ,” *Journal of Magnetism and Magnetic Materials 320* e702–e707, 2008.

[2] Z. Oudni, H. Mohellebi, M. Féliachi, “Effect of Aluminum Layer on Induction Heating Control Case Study Using Finite Elements Method," *Journal of electrical systems* 2009.

[3] B. Kane, *Contribution à la modélisation des phénomènes de percolation électrique dans les matériaux à structures complexes : application au soudage par induction des matériaux composites pour l’industrie aéronautique* , Ph.D. dissertation, Nantes Université, 2019.

[4] A. Demier, J. Giusti, S. Naudin, B. Oville, P. Perichon , F. Petit, T. Waeckerle, and T. Wery, “Etude magnétothermique d’un alliage à bas point de Curie en cuisson par induction ," *Symposium de Génie Electrique* 2016.

[5] O. Messal, F. Sixdenier, L. Morel, N. Burais, “Thermal behavior of Iron-Nickel-Chromium Alloys and Correlation with Magnetic and Physical Properties-Part A : Static Effects Modeling," *Journal : Transactions on Magnetics - Conferences.,* 2013.

[6] A. E. Umenei, Y. Melikhov, and D. C. Jiles, “Models for Extrapolation of Magnetization Data on Magnetic Cores to High Fields ," *IEEE Transactions on Magnetics,* 2011.

[7] M. Belkadi, *Contribution à l’homogénisation multi-échelle des propriétés électromagnétiques des matériaux en poudres de fer* , Ph.D. dissertation, Nantes Université, 2009.